INNSPUB

Journal of Biodiversity and Environmental Sciences | JBES
ISSN: 2220-6663 (Print); 2222-3045 (Online)
Website: https://www.innspub.net
E-mail contact: info@innspub.net
Vol. 27, Issue: 6, p. 102-113, 2025

RESEARCH PAPER OPEN ACCESS

Optimizing mannings roughness coefficient for hydraulic modelling: An application for Pinacanauan De Tuguegarao watershed, Philippines

Policarpio L. Mabborang Jr.*, Jonathan A. Saturno, Jose D. Guzman, James B. Cabildo, Rio Jay R. Banan, Luzviminda M. Adolfo

Cagayan State University, Tuguegarao City, Cagayan, Philippines

Key words: Flooding, Hydrologic simulation, Hydraulic simulation, HEC-HMS, Pinacanauan de Tuguegarao watershed

Received: 02 December, 2025 **Accepted:** 09 December, 2025 **Published:** 13 December, 2025

DOI: https://dx.doi.org/10.12692/jbes/27.6.102-113

ABSTRACT

Flooding poses a significant threat to Pinacanauan de Tuguegarao watershed, with increasing frequency of occurrences prompting the urgent need for enhanced flood forecasting through model calibration and validation. The city's most severe flood event was recorded during Typhoon Ulysses, which served as the basis for calibrating the hydrologic and hydraulic models of the Pinacanauan de Tuguegarao watershed. Using HEC-HMS, the hydrologic simulation optimized Clark's unit hydrograph parameters (time of concentration and storage coefficient) and SCS curve number loss method parameters (curve number and initial abstraction), achieving precise simulation of observed hydrographs. Calibration of the hydraulic model using TUFLOW adjusted Manning's roughness coefficient iteratively, settling on depth-varying values from 0.002 at 3.5 meters to 0.4 at 4 meters, with the model accurately predicting stage heights and discharge rates as evaluated by NSE, PBIAS, RMSE, and RSR metrics. Validation during Typhoons Paeng and Tisoy demonstrated the model's proficiency in predicting extreme and moderate flood events, although with tendencies to overestimate minor floods. The calibrated model subsequently facilitated the development of a flood model for Typhoon Ulysses and an early warning system based on river stage heights, enhancing decision-making and communication for disaster preparedness and response in Tuguegarao City.

***Corresponding Author:** Policarpio L. Mabborang Jr. ✉ pol_jr@yahoo.com

INTRODUCTION

Floods are among the most frequent natural disasters globally, causing substantial damage and affecting millions of people annually. Approximately 30% of financial losses from natural disasters are attributed to floods (Abbott *et al.*, 1986). From 1998 to 2017, floods affected up to 2 billion people worldwide, particularly those in flood-prone areas lacking resilience or early warning systems (World Health Organization, 2022).

The Philippines, highly vulnerable to natural disasters, has seen significant impacts, with 74% of its population and 60% of its land area exposed to various threats. Since 1990, the country has faced 565 disasters, resulting in 70,000 casualties and $23 billion USD in damages (World Bank, 2021). Typhoons are frequent due to its location in the Northwestern Pacific Basin, with storms accounting for 46.94% and flooding for 23.13% of recorded natural disasters (World Bank, 2021).

Urban areas, with dense infrastructure and high population migration, are particularly vulnerable to natural disasters like floods (Natarajan and Radhakrishnan, 2020). The Cagayan River Basin, the largest in the Philippines at 27,493.49 km², includes critical watersheds like Pinacanauan de Tuguegarao, draining from Sierra Madre mountains into the floodplain of Peñablanca and Tuguegarao City (Department of Environment and Natural Resources, n.d.).

Hydrodynamics, crucial for understanding fluid behavior, involves mathematical modeling of properties such as velocity and viscosity, governed by differential equations (Le Méhauté, 1927). Advanced river hydraulic models simulate fluid dynamics using physics principles like the Navier-Stokes equation, benefiting flood and tidal analysis in rivers and coastal areas (Hosseiny *et al.*, 2020; Syme, 1990). Analyzing and studying hydrological models suitable to specific watershed conditions is vital for enhancing their accuracy and relevance (Ngoc *et al.*, 2011; Noh *et al.*, 2018).

Study of the DREAM Flood Forecasting have been crucial for predicting floods in the Cagayan River Basin, but there's a lack of a validated model specifically for Pinacanauan de Tuguegarao. Current challenges include insufficient hydrological data, which can compromise the reliability of flood predictions (Alfonso *et al.*, 2019; Garcia *et al.*, 2016). This study aims to develop a calibrated and validated hydrologic and hydraulic model for Pinacanauan de Tuguegarao, focusing on accurate representation of hydrological parameters and Manning's roughness coefficient through simulations, particularly in response to events such as Typhoon Ulysses.

MATERIALS AND METHODS

Description of the study area

The Pinacanauan de Tuguegarao watershed is one of the sub-basins of the Cagayan River basin. It is located at 17°46'15.88"N, 121°43'1.46"E (1); 17°46'9.93"N, 122° 3'41.85" E (2); 17°30'28.35"N, 121°43'6.13"E (3); 17°30'21.48"N, 122° 5'27.40" E (4) shown in Fig. 1.

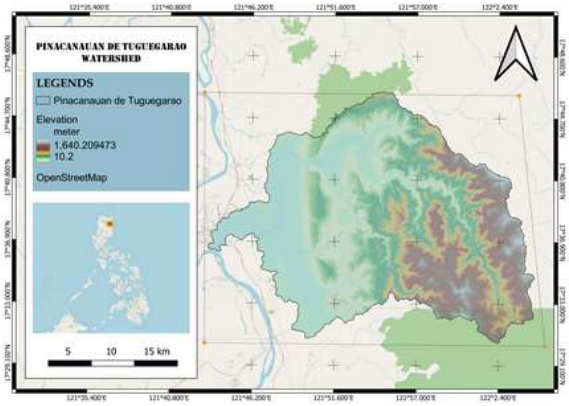

Fig. 1. Pinacanauan de Tuguegarao watershed (Source: OpenStreetMap)

Its catchment area is 650.66 km², majority lies within the municipality of Peñablanca, with the outlet located in Tuguegarao City. A small portion of the watershed is also covered by San Pablo, Isabela. The Pinacanauan River primarily flows through the municipality of Peñablanca and discharges into the Cagayan River. The stream gage is located at Josefa Bridge, Larion, Tuguegarao City—the study area experiences Type III climate which seasons are not very distinct. The climate is relatively dry from

November to April, transitioning to wet conditions for the remainder of the year. The periods of maximum rainfall are not clearly defined, with a brief dry season lasting only three months.

Topography and land cover/use of Pinacanauan de Tuguegarao

The Digital Elevation Model (DEM) of the study site was obtained from the National Mapping Resource Information Authority (NAMRIA) in the form of an Interferometric Synthetic Aperture Radar (IFSAR) with a resolution of 5 meters as shown in Fig. 2. The land cover shapefile of the study area was from NAMRIA presented in Fig. 3. The DEM and Land cover of the model were clipped using the QGIS to remove permanently dry or high-elevation areas. Minimizing the extent of the model boundary and computational area saves computational time.

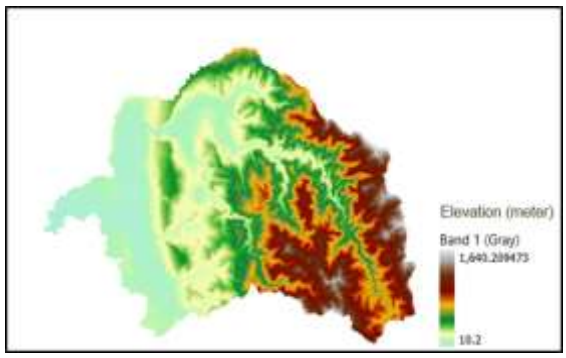

Fig. 2. Topography of Pinacanauan de Tuguegarao watershed (2015) (Source: NAMRIA)

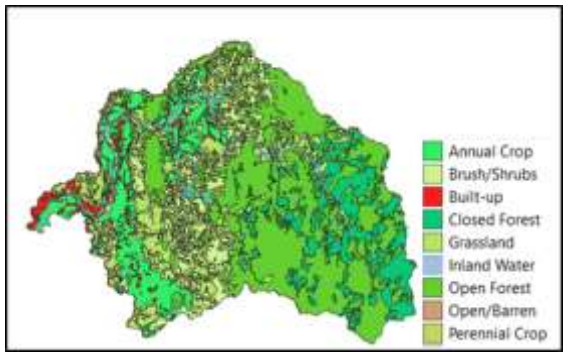

Fig. 3. Land Cover/Land Use of Pinacanauan de Tuguegarao (2020) (Source: NAMRIA)

Methodologic framework

The method applied by the researcher in this study was shown in Fig. 4. The hydrologic simulation was conducted by processing the rainfall data of a typhoon event and processing watershed properties, then hydraulic simulation was executed.

Fig. 4. Operational framework of hydrologic and hydraulic calibration and validation

Hydrologic model development

HEC-HMS is a hydrologic modeling software developed by the US Army Corps of Engineers at the Hydrologic Engineering Center. The study utilized four components to simulate the basic hydrologic process. For the study, rainfall-runoff modeling using Clark's Unit Hydrograph, infiltration loss using SCS curve number, baseflow using constant monthly, and routing method using Muskingum-Cunge were executed.

The operational workflow of HEC-HMS is shown in Fig. 4. Executing a hydrologic model using HEC-HMS software, the project must contain basin files, meteorological models, time series data, and terrain data. In the 4.11 version of HEC-HMS, GIS processing allows users to delineate watersheds and conduct hydrologic processing. Parameters for the transform, routing, loss, and baseflow were defined to compute the output hydrograph. The observed flow during Typhoon Ulysses (November 1 – 16, 2020) was derived from the stage height recorded at Josefa Bridge. Rainfall data corresponding to Typhoons Ulysses served as input parameters, allowing for the examination of whether the modified hydrological parameters can accurately reproduce the observed stage height and discharge rates.

The infiltration loss component was the SCS curve number method which computes the amount of

rainfall that discharges on the watershed and determines the volume of rainfall that infiltrates the soil (Soomro *et al.*, 2019). The Curve Number parameters for each sub-basin were determined based on the land cover and soil map of the watershed. In HEC-HMS, the SCS-CN method requires the curve number and initial abstraction (mm) of each sub-basin. The values of the curve number are based on the Technical Report 55 (TR-55). The estimation of the initial abstraction (Ia) was calculated by multiplying the maximum retention (S) by 0.2.

The transform method utilized was Clark's unit hydrograph to determine the direct runoff volume and the attenuation of the magnitude of the discharge as the excess was stored in the watershed. For Clark's unit hydrograph model, the time of concentration and storage coefficient (T_c and R) were estimated for each sub-basin by applying the TR-55 method (Santillan *et al.*, 2013).

$$T_c = 2.2 * \left(\frac{L * L_c}{\sqrt{Slope_{10-85}}}\right)^2 \quad \text{Equation 1}$$

Where:

T_c is the time of concentration (hrs)

L is the longest flow path (mi)

L_c is centroidal flow path (mi)

$Slope_{10\text{-}85}$ is the average slope of the flow path represented by 10 to 85 percent of the longest flow path (ft/mi)

The calculated direct runoff and baseflow hydrographs for each watershed were then routed through reaches towards the main outlet of the Pinacanauan de Tuguegarao watershed through the Muskingum-Cunge method. The channels were selected as trapezoidal in shape. The manning's roughness coefficients were defined. The bottom widths of the channels were obtained through the spatial imagery of the study site.

Hydraulic simulation

Hydraulic simulation was conducted using TUFLOW software. The simulation was solved using the full 2D hydrodynamic free surface flow equations and solved using the CPU-based implicit solver, unconditional, second-order spatial solver (Barton *et al.*, 2015). The preparation of inputs such as land cover layers, the definition of the boundary condition location, and the model domain was done using QGIS. The control files were coded using Notepad++ to define the parameters and shapefiles read by the solver. The roughness coefficient that was integrated into the land cover data was defined using the industry-based Manning's coefficient. A sensitivity analysis determines how the assigned roughness value affects the model's behavior. The hydrograph of typhoon Ulysses defines the upstream boundary, and the downstream defines the free outflow condition with an initial water level. The roughness coefficient values of each material file were determined by using industry-based values. Since the stream gauge is located at Josefa Bridge, the inundated area was limited at the Josefa Bridge at Larion to the confluence of Pinacanauan de Tuguegarao and Cagayan River. The calibrated flood discharge was the input for the inundation of the Pinacanauan de Tuguegarao watershed.

Calibration and validation

One of the most essential procedures in generating a hydraulic model is calibration, including the selection of calibration parameters and boundary conditions (Kuhanestani *et al.*, 2022). The roughness coefficient is the most common and sensitive parameter to calibrate hydraulic models. The stage heights and discharge curves during Typhoon Ulysses on November 1-16, 2023, were used for calibration. The stage height data and discharge curve during Typhoon Tisoy on November 24, 2019, to December 6, 2019, and Typhoon Paeng on October 28, 2022, to November 2, 2022, ware used for the validation process.

Performance evaluation

The measures of accuracy of a hydrological model to evaluate the performance of the model before and after the calibration including the validation were presented by Garcia *et al.* (2016). The Nash-Sutcliffe Coefficient Value of Model Efficiency (NSE), percent

bias (PBIAS), and RMSE-observations standard deviation ratio (RSR). Moriasi *et al.* provided guidelines to systematically quantify the HEC-HMS model performance (Santillan *et al.*, 2013) (Table 1).

Table 1. Performance ratings (Source: Moriasi *et al.*, 2007, adopted in Santillan *et al.* (2013)

Performance rating	Statistics		
	NSE	PBIAS	RSR
Very good	0.75 < NSE ≤ 1.00	PBIAS < ± 10	0.00 < RSR ≤ 0.50
Good	0.65 < NSE ≤ 0.75	± 10 ≤ PBIAS < ± 15	0.50 < RSR ≤ 0.60
Satisfactory	0.50 < NSE ≤ 0.65	± 15 ≤ PBIAS < ± 25	0.60 < RSR ≤ 0.70
Unsatisfactory	NSE ≤ 0.50	PBIAS ≥ ± 25	RSR > 0.70

Nash-sutcliffe efficiency (NSE)

Nash-Sutcliffe Efficiency (NSE) is a standardized metric used to assess the relative magnitude of noise (residual variance) in comparison to the information contained in the measured data variance (Nash and Sutcliffe, 1970).

$$NSE = 1 - \frac{\sum_{i=1}^{n}(Y_i^{obs} - Y_i^{sim})^2}{\sum_{i=1}^{n}(Y_i^{obs} - Y^{mean})^2} \quad \text{Equation 2}$$

Where:

NSE is the Nash-Sutcliffe Efficiency

Y_i^{obs} is the observed data

Y_i^{sim} is the simulated data

Y^{mean} is the mean of the observed data

The NSE ranges from −∞ to 1, where 1 indicates a perfect match between simulated and observed data, and values closer to 0 or negative indicate poorer model performance. It's widely used due to its ability to provide a comprehensive assessment of model fit to the hydrograph (Kuhanestani *et al.*, 2022).

Percent bias (PBIAS)

Percent Bias (PBIAS) is the measure of the average tendency of the simulated data to be smaller or larger than the actual data (Gupta *et al.*, 1999).

$$PBIAS = \frac{\sum_{i=1}^{n}(Y_i^{obs} - Y_i^{sim}) * 100}{\sum_{i=1}^{n}(Y_i^{obs})} \quad \text{Equation 3}$$

Where:

PBIAS is the deviation of evaluated data, expressed as a percentage.

Y_i^{obs} is the observed data

Y_i^{sim} is the simulated data

The optimal value for PBIAS is 0, a lower magnitude indicates an accurate model simulation. A positive PBIAS value indicates an underestimation bias in the simulated model, while a negative value suggests an overestimation bias. PBIAS is valued for its ability to quantify water balance errors and can be extended to assess load errors serving as an important indicator in evaluating hydrological model accuracy (Sevat and Dezetter, 1991).

Root mean square error (RMSE)

The Root Mean Square Error (RMSE) serves as a metric for quantifying the absolute differences between observed and simulated values. This statistical index provides a numerical measure, ranging from 0 to +∞ (Eslamian and Eslamian, 2023). A lower RMSE suggests a closer fit between the model and the real-world data, indicating better predictive accuracy.

$$RMSE = \sqrt{\frac{\sum(S-O)^2}{n}} \quad \text{Equation 4}$$

Where:

RMSE is the root mean square error

S is the simulated value

O is the observed value

n is the number of observations or data points

RMSE-observations standard deviation ratio (RSR)

The RSR statistic standardizes the Root Mean Square Error (RMSE) by utilizing the standard deviation of the observations (Kuhanestani *et al.*, 2022). The RSR metric ranges from the ideal value of 0, indicating zero residual variation or RMSE and hence a perfect model simulation, to greater positive value.

$$RSR = \sqrt{\frac{\sum(S-O)^2}{\sum(O-\bar{x})^2}} \quad \text{Equation 5}$$

Where:

RSR is the root mean square error

S is the simulated value
O is the observed value
$\bar{x}$ is the averaged observed values

RESULTS AND DISCUSSION

Hydrologic simulation results

This study focused on the calibration and validation of a hydrologic and hydraulic model for the Pinacanauan de Tuguegarao watershed using the HEC-HMS software and TUFLOW.

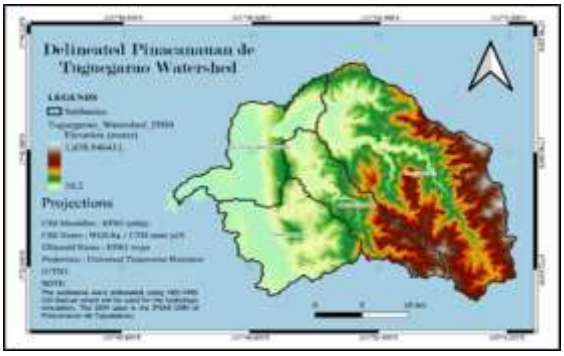

Fig. 5. Delineated Pinacanauan de Tuguegarao watershed

The Pinacanauan de Tuguegarao watershed was divided into four sub-basins using the HEC-HMS tool shown in Fig. 5. These sub-basins, which encompass the watershed's major tributaries, are the Lapi sub-basin, Natallad sub-basin, Abaca sub-basin, and lower Pinacanauan sub-basin. The Lapi sub-basin, which contains the upper Pinacanauan de Tuguegarao River, is the largest, covering 306.74 km² (48.23% of the watershed). It captures the most rainfall, producing the largest runoff volume, and has the longest lag time. The Natallad sub-basin, containing the Natallad Creek, is the smallest at 101.85 km² (16.01% of the watershed) and captures the least rainfall. The Abaca sub-basin, containing the Abaca Creek, covers 120.38 km² (18.93% of the watershed). The lower Pinacanauan sub-basin, which includes the mid and lowerPinacanauan River, covers 107 km² (16.82% of the watershed). These sub-basins were characterized in HEC-HMS to determine its different flowpath lengths which are parameter for the calculation of time of concentration for the rainfall transform.

Geospatial sub-basin characterization was computed in the HEC-HMS software. The longest flowpath, a measurement from the sub-basin outlet to the most hydraulically remote upstream point, is crucial for determining the time of concentration. The Lapi sub-basin, with a longest flowpath of 49.50 km, indicated the longest time of concentration, while the Abaca sub-basin, with a 28.17 km flowpath, had the shortest time of concentration. The Natallad and Lower Pinacanauan sub-basins had flowpaths of 41.43 km and 35.63 km, respectively. The slope of these flowpaths varied, with Natallad having the steepest slope at 0.04085, followed by Abaca (0.02576), Lapi (0.02371), and Lower Pinacanauan (0.01628), indicating the least steep slope.

Centroidal flowpath lengths, extending from the outlet along the longest flowpath to the centroid of the sub-basin, were 22.1 km for Lapi, 21.58 km for Natallad, 9.0715 km for Abaca, and 14.87 km for Lower Pinacanauan. The slopes of these centroidal flowpaths showed that Natallad had the steepest slope at 0.00872, with Lapi at 0.006, and both Abaca and Lower Pinacanauan at approximately 0.00175, indicating relatively less steep terrain.

The 10-85 flowpath, another measure of flowpath characteristics, provided additional insights into the elevation gradient and hydrologic response. Basin slope and relief further detailed the terrain's steepness and elevation differences. The elongation ratio, determining the shape of the sub-basins, suggested that Natallad, Lower Pinacanauan, and Lapi were elongated, while Abaca was closer to circular, potentially leading to faster peak flow times.

Drainage density, which evaluates the extent of stream length relative to the basin area, showed values of 0.1173 for Lapi, 0.2072 for Natallad, 0.0911 for Abaca, and 0.2945 for Lower Pinacanauan.

Optimized parameters and calibration result of the hydrologic simulation

The comparison between output of HEC-HMS, the simulated and observed flood hydrographs for the

Pinacanauan de Tuguegarao watershed was presented in Fig. 6. The observed flow rates show a consistent upward trend until November 10, 2020, followed by an abrupt change and subsequent decline. The peak discharge occurs on November 13, 2020, with a peak discharge rate of 443.7 m^3/s and a total accumulated volume of 341.91 * 10^6 m^3. In contrast, the simulated hydrograph initially displays a flat curve until November 6, 2020, followed by an increase leading to a peak discharge of 448.4 m^3/s on November 12, 2020. The simulated hydrograph declines faster than the observed one. While the simulated model accurately predicts the peak discharge and slope, it tends to overestimate discharge rates and predict an earlier time to peak by 6 hours. The simulated hydrograph exhibits a sinusoidal discharge rate pattern compared to the observed flow rate, indicating potential differences in sub-basin drainage pattern.

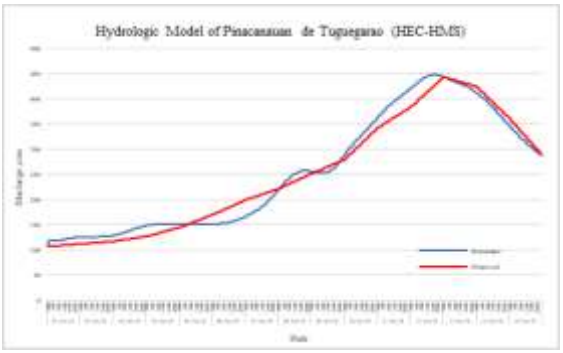

Fig. 6. Simulated vs observed flood hydrograph of Pinacanauan de Tuguegarao watershed

The study identifies 8 parameterizations each for Clark's unit hydrograph transform method and the SCS curve number loss method shown in Table 2. Sensitivity analysis revealed that the storage coefficient, SCS curve number, and SCS initial abstraction were the most sensitive parameters, while the time of concentration remained unchanged.

Table 2. Optimized parameters in Hydrologic simulation

Sub-basin	Parameter	Unit	Initial value	Optimized value
Lapi Subbasin	Clark Unit Hydrograph - Storage Coefficient	HR	71.35954	61.645
	Clark Unit Hydrograph - Time of Concentration	HR	25.67584	25.67584
Natallad Subbasin	Clark Unit Hydrograph - Storage Coefficient	HR	64.504	84.421
	Clark Unit Hydrograph - Time of Concentration	HR	22.576	22.576
Abaca Subbasin	Clark Unit Hydrograph - Storage Coefficient	HR	51.649	45.429
	Clark Unit Hydrograph - Time of Concentration	HR	18.07707	18.07707
Lower Pinacanauan	Clark Unit Hydrograph - Storage Coefficient	HR	78.68817	22.581
	Clark Unit Hydrograph - Time of Concentration	HR	27.54086	27.54086
Lapi Subbasin	SCS Curve Number	mm	82	99
	SCS Curve Number – Initial Abstraction	mm	16.4	25.099
Natallad Subbasin	SCS Curve Number	mm	55	93.921
	SCS Curve Number – Initial Abstraction	mm	11	68.883
Abaca Subbasin	SCS Curve Number	mm	75	66.747
	SCS Curve Number – Initial Abstraction	mm	15	0.01
Lower Pinacanauan	SCS Curve Number	mm	95	99
	SCS Curve Number – Initial Abstraction	mm	19	0.01

Optimization results indicated changes in storage coefficients for each sub-basin presented in Table 2. In the Lapi sub-basin, the storage coefficient decreased from 71.36 hours to 61.65 hours, suggesting faster runoff release and resulting in a higher and earlier peak flow. Conversely, the Lower Pinacanauan sub-basin's storage coefficient significantly decreased from 78.69 hours to 22.581 hours, leading to a steeper hydrograph shape and higher peak discharge. The Abaca sub-basin's storage coefficient reduced from 51.65 hours to 45.43 hours, intensifying the hydrograph and minimizing the time of concentration. Lastly, the Natallad sub-basin's storage coefficient increased from 65.50 hours to 84.42 hours, indicating a more attenuated hydrograph with decreased peak flow and a longer time of concentration.

The optimization results showcased the Nash-Sutcliffe Efficiency (NSE), Percent Bias (PBIAS), and Root Mean Square Error (RMSE) values in Table 3. The optimized model demonstrates

exceptional performance, achieving an NSE of 0.972, indicating that it explains 97.2% of the variance in the observed data, signifying excellent precision in simulating the observed hydrograph. Additionally, the low PBIAS value of 0.91% suggests minimal bias, with model predictions closely matching actual values. The low RMSE value of 0.2 further emphasizes the model's accuracy and reliability, indicating small differences between observed and predicted values. Overall, these statistical indices affirm that the calibrated model accurately fits the observed hydrograph.

Table 3. Calibration result of the hydrologic simulation

Statistical Index	Rating	Remarks
NSE	0.972	Very Good
PBIAS	0.91%	Very Good
RMSE	0.2	Excellent

Hydraulic Simulation and Calibration of Pinacanauan de Tuguegarao

The comparison of the simulated and observed stage heights for the Pinacanauan de Tuguegarao River in Fig. 7, indicates significant accuracy improvements with a depth-varying roughness coefficient. The simulated model closely mimics the rising limb of the hydrograph, with minor initial overestimation of lower stage heights. Peak stage heights show a negligible underestimation, while the falling limb demonstrates strong correlation between simulated and observed data. Conversely, the simulated and observed discharge presented in Fig. 8 reveal deviations in model output. Despite compensating for early overestimation during higher discharge periods, the model underestimates peak discharge. Both simulated and observed discharge peaks occur simultaneously, with the simulated model underestimating peak discharge by 40.74 m^3/s.

The calibrated Manning's roughness coefficient for the Pinacanauan de Tuguegarao watershed was determined to be depth-varying, with optimal values of 0.002 for depths up to 3.5 meters and 0.4 for depths exceeding 4 meters. The calibrated hydraulic model achieved favorable performance ratings, with stage height results yielding NSE, RMSE, RSR, and PBIAS values of 0.94, 0.37, 0.24, and -1.28%, respectively. Despite a slight overestimation, the model's performance is considered very good. Similarly, discharge results produced NSE, RMSE, RSR, and PBIAS values of 0.97, 18.29, 0.16, and 2.18%, respectively, indicating very good performance despite some underestimation in simulated discharge (Table 4).

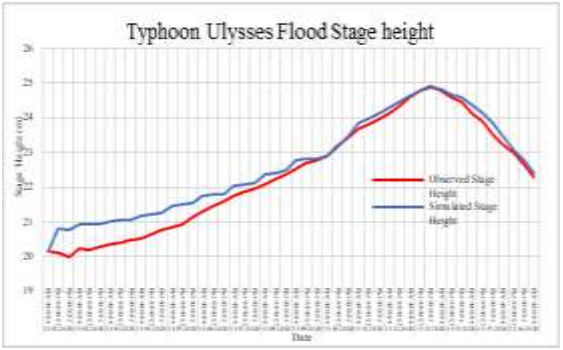

Fig. 7. Stage height curve of observed and simulated hydraulic model during Typhoon Ulysses

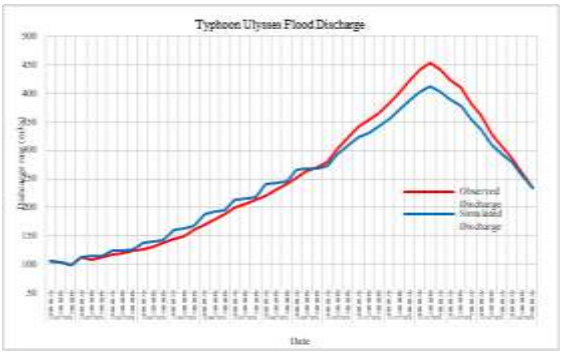

Fig. 8. Discharge curve of observed and simulated hydraulic model Typhoon Ulysses

Table 4. TUFLOW performance rating during calibration of Typhoon Ulysses

Typhoon Ulysses	Manning's Coefficient	Statistical Index	Rating	Remarks
Calibrated Stage height	3.5m,0.002 –4m,0.4	NSE	0.94	VG
		RMSE	0.37	-
		RSR	0.24	VG
		PBIAS	-1.28	VG
Calibrated discharge		NSE	0.97	VG
		RMSE	18.29	-
		RSR	0.16	VG
		PBIAS	2.18	VG

*VG = Very Good

Validation result

The validation results for Typhoon Paeng's flooding data indicate that the simulated model slightly underestimated observed stage heights, with a peak stage height discrepancy of 0.43 meters occurring 2 hours later than observed shown in Fig. 9. However, the discharge curves in Fig. 10 demonstrated a strong correlation between simulated and observed data, with the simulated model accurately capturing peak discharge rates with minimal discrepancy.

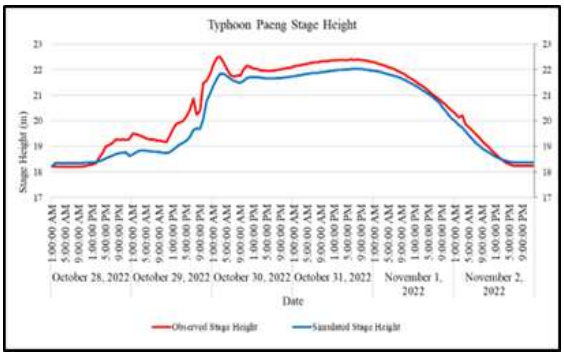

Fig. 9. Stage height curve of observed and simulated hydraulic model during Typhoon Paeng

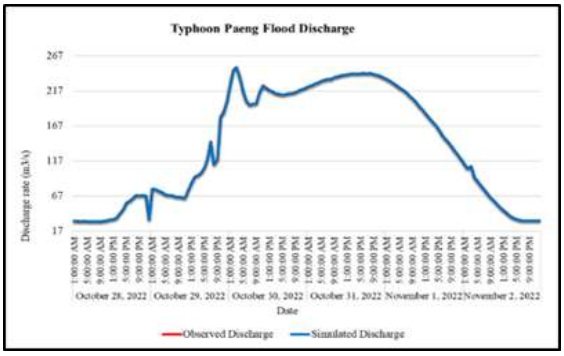

Fig. 10. Discharge curve of observed and simulated hydraulic model during Typhoon Paeng

Table 5. presents the performance ratings for stage height and discharge simulations during Typhoon Paeng were high, with NSE values of 0.92 and 0.99, respectively, indicating superior model performance in replicating observed data. RMSE and RSR values further supported the accuracy and fit of the model, while PBIAS values indicated negligible bias in both stage height and discharge predictions.

Table 5. TUFLOW performance rating during model validation using Typhoon Paeng

Typhoon Paeng	Manning's Coefficient	Statistical Index	Rating	Remarks
Calibrated Stage height	3.5 m,0.002 – 4 m,0.4	NSE	0.92	VG
		RMSE	0.51	-
		RSR	0.27	VG
		PBIAS	1.56	VG
Calibrated discharge		NSE	0.99	VG
		RMSE	.16	-
		RSR	0.004	VG
		PBIAS	-0.04	VG

*VG = Very Good

Fig. 11 and 12 presented the validation results during Typhoon Tisoy which characterized as a low flooding event. The simulated stage height curves initially overestimated observed data at lower thresholds but underestimated peak stage height. The simulated peak occurred 5 hours earlier than observed, with a minimal underestimation of 0.28 meters. Discharge curves exhibited a stronger correlation, with the simulated model closely resembling observed data, although underestimating by 5.59 m3/s (Table 6).

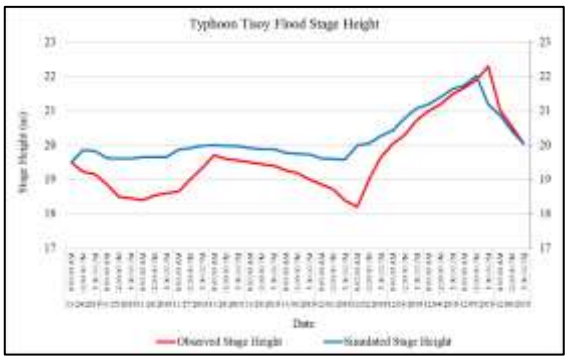

Fig. 11. Stage height curve of observed and simulated hydraulic model during Typhoon Tisoy

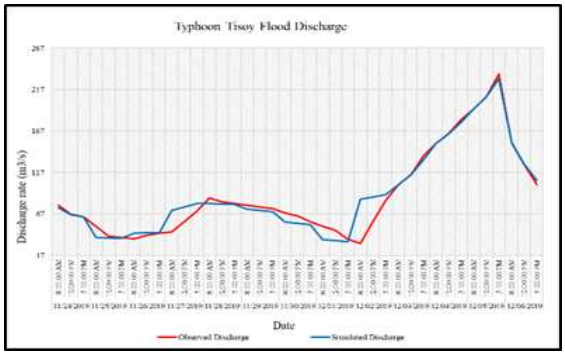

Fig. 12. Discharge curve of observed and simulated hydraulic model Typhoon Paeng

Table 6. TUFLOW performance rating during model validation using Typhoon Tisoy

Typhoon Tisoy	Manning's Coefficient	Statistical Index	Rating	Remarks
Validation Stage height	3.5 m,0.002 – 4 m,0.4	NSE	0.50	Satisfactory
		RMSE	0.76	-
		RSR	0.71	Unsatisfactory
		PBIAS	-2.83	VG
Validation discharge		NSE	0.94	VG
		RMSE	12.36	-
		RSR	0.23	VG
		PBIAS	-1.39	VG

*VG = Very Good

Performance ratings for stage height and discharge simulations yielded NSE values of 0.50 and 0.94, respectively, indicating satisfactory and very high levels of accuracy. While stage height simulation showed average accuracy, discharge simulation performed well, with low RMSE and PBIAS values suggesting slight overestimation. Despite moderate performance for stage height, the model demonstrated reliable discharge predictions during Typhoon Tisoy, highlighting its suitability for higher flooding events but indicating room for improvement in lower flooding scenarios.

Flood inundation map of Typhoon Ulysses in Tuguegarao City

The flooded areas during Typhoon Ulysses, as illustrated in the inundation map in Fig. 13. The analysis reveals that barangays located adjacent to the Pinacanauan River and Caritan Creek were particularly prone to flooding. Centro 9 was identified as the most affected, with 85.32% of its 36.2 ha land area inundated, and Centro 10 with 80.50% of its 58.14 ha land area inundated.

Moderate flooding was observed in barangays such as Balzain West with 60.38% of its 34.97 ha land area inundated, Balzain East with 56.45% of its 94.90 ha land area inundated, Lario Bajo with 46.76% of its 282.51 ha land area inundated.

Low flooding barangays are Capatan with 29.31% of its 207.61 ha land area inundated, Centro 5 with 22.74% of its 26.18 ha land area inundated, Centro 1 with 19.26% of its 18.19 ha land area inundated, Libag Norte with 17.86% oof its 369.49 ha land area inundated, Tanza with 52.86% of its 24.46 ha land area inundated, and Larion Alto with 15.79% of its 452.65 ha land area inundated.

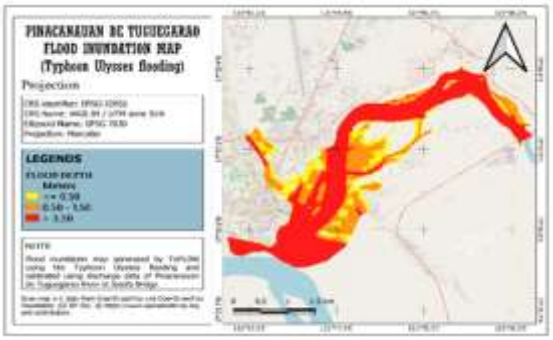

Fig. 13. Flood inundation map of the calibrated model during Typhoon Ulysses

Out 49 barangays, 32 of which are not affected by the flooding from Pinacanauan de Tuguegarao during typhoon Ulysses.

The flood inundation during Typhoon Ulysses in Pinacanauan de Tuguegarao and including backflow from Cagayan River was illustrated in the inundation map in Fig. 14. It was analyzed that 12 out of 49 barangays of Tuguegarao were within the 67% to 100% inundation based on the land area. These barangays are Centro 9, Centro 10, Balzain East, Cataggaman Viejo, Centro 1, Buntun, Balzain West, Cataggaman Pardo, Annafunan West, Centro 5, Cataggaman Nuevo, and Annafunan East.

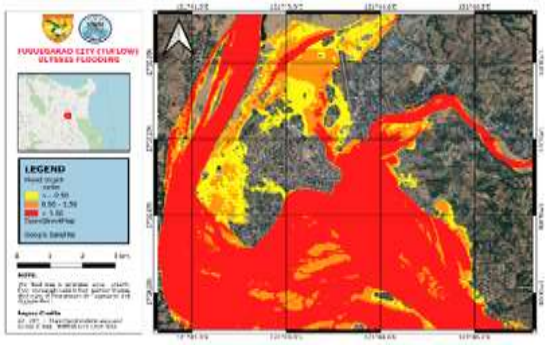

Fig. 14. Flood inundation map of the calibrated including backflow during Typhoon Ulysses

18 out of the 49 barangays were considered to be moderate flooding barangay with an inundation

percentage of 33% to 66%. These barangays are Atulayan Sur, Linao East, Libag Sur, Atulayan Norte, Ugac Sur, Linao West, Caritan Norte, Larion Bajo, Gosi Norte, Libag Norte, Pallua Sur, Tanza, Tagga, Gosi Sur, Pallua Norte, Bagay Capatan, and Linao Norte.

11 out of 49 barangays were low flooding barangay with an inundation level of 0.01% to 32%. These are Caritan Centro, Dadda, Pengue-Ruyu, Carig Sur, Larion Alto, Caggay, Centro 6, Caritan Sur and Carig Norte. It is noticeably that flooded area of Carig Sur, Pallua Norte, Bagay, Larion Alto, Larion Bajo, Libag Norte, and Dadda were mainly floodplains.

Early warning recommendations

Early warning systems through flood forecasting are vital for mitigating the devastating impacts of floods on communities, infrastructure, and economies. These systems play a crucial role in enhancing preparedness, enabling timely evacuations, and reducing casualty and property damage. Through the calibration of Pinacanauan de Tuguegarao, flood forecasting of future flooding can aid in developing a more robust and comprehensive early warning system.

During Typhoon Ulysses, data from Josefa Bridge indicated that at 21 meters, warnings for potential flooding should be issued. At 22 meters, high-risk barangays should prepare for evacuation, with warnings for moderate-risk areas. At 23 meters, high-risk areas should begin voluntary evacuation, while moderate-risk areas should prepare. At 24 meters, forced evacuations should be implemented.

Timely evacuations, allow residents to move to safer areas, reducing casualties, especially in densely populated barangays such as Balzain East, Balzain West, and Caritan Norte.

CONCLUSION

The study of hydrological and hydraulic behaviors, alongside the calibration and validation of simulation models, has provided significant insights into the flood dynamics of the Pinacanauan de Tuguegarao watershed. Optimized Clark's Unit Hydrograph and SCS curve number hydrological parameters accurately predicted the hydrograph of Typhoon Ulysses. The study found that the Manning's roughness coefficient varied with depth, optimal at 0.002 for depths up to 3.5 meters and 0.4 for deeper areas, enhancing hydraulic simulation accuracy. Integration of Cagayan River backflow data improved flood extent understanding, supporting targeted flood management strategies. The model performed excellently in predicting extreme and moderate flooding, with precise simulations of stage heights and discharge rates during typhoons Ulysses, Paeng, and Tisoy. However, during low flooding events, variability in predictions was noted. The study highlights the model's potential as an early warning system for extreme flooding, offering crucial insights into flood magnitude and extent for preparedness, evacuation, and damage estimation in future flood events.

ACKNOWLEDGEMENTS

This study was realized through the support of the Integrated Assessment and Analysis of Hydraulic Assets for Sustainable and Resilient Flood Control Infrastructure Project under the program Smart Water Infrastructure Management (SWIM) RandD Center. Special thanks to the DOST – Science for Change (S4C) Program, Niche Centers in the Regions for RandD (NICER) Program. The authors also express gratitude to the National Mapping Resource Information Authority (NAMRIA) for providing datasets for the DEM and Land Cover/Use, Department of Public Works and Highways (DPWH) Hydrologic section for the Stage heights datasets, and Philippine Atmospheric, Geophysical and Astronomical Services Administration (PAGASA) for the rainfall datasets.

REFERENCES

Abbott MB, Bathurst JC, Connell PE, Rasmussen JR. 1986. An introduction to the European hydrologic system—Système Hydrologique Européen (SHE): history of a physically based, distributed modeling system. Journal of Hydrology **87**, 45–59.

Alfonso C, Sundo M, Zafra R, Velasco P, Aguirre J, Madlangbayan M. 2019. Flood risk assessment of major river basins in the Philippines. International Journal of GEOMATE **16**, 201–208.

Barton J, Babister M, Burston J. 2015. TUFLOW Classic / TUFLOW HPC—user manual. https://www.tuflow.com/

Department of Environment and Natural Resources (DENR). n.d. Cagayan River Basin. River Basin Control Office. https://riverbasin.denr.gov.ph/river/cagayan

Eslamian S, Eslamian F. 2023. Handbook of hydroinformatics, volume III: water data management best practices. Elsevier, Inc.

Garcia FC, Retamar AE, Javier JC. 2016. Development of a predictive model for on-demand remote river level nowcasting: case study in Cagayan River Basin, Philippines. Institute of Electrical and Electronics Engineers Proceedings, 3275–3279.

Gupta HV, Sorooshian S, Yapo PO. 1999. Status of automatic calibration for hydrologic models: comparison with multilevel expert calibration. Journal of Hydrologic Engineering **4**, 135–143.

Hosseiny H, Nazari F, Smith V, Nataraj C. 2020. A framework for modeling flood depth using a hybrid of hydraulics and machine learning. Scientific Reports **10**, 1–13.

Kuhanestani R, Kowsar K, Bhardwaj A. 2022. Development of a 2D hydraulic model for assessing flood hazards in urban areas. Natural Hazards Review **23**(2), 05021005.

Le Méhauté B. 1976. An introduction to hydrodynamics and water waves. Springer Science+Business Media, California.

Nash JE, Sutcliffe JV. 1970. River flow forecasting through conceptual models. Journal of Hydrology **10**, 282–290.

Natarajahan S, Radhakrishnan N. 2020. An integrated hydrologic and hydraulic flood modeling study for a medium-sized ungauged urban catchment area: a case study of Tiruchirappalli City using HEC-HMS and HEC-RAS. Journal of the Institution of Engineers (India) **101**, 381–398.

Ngoc TA, Chinh LV, Hiramatsu K, Harada M. 2011. Parameter identification for two conceptual hydrological models of Upper Dau Tieng River watershed in Vietnam. Journal of the Faculty of Agriculture, Kyushu University **56**(2), 335–341.

Noh J, Lee J, Shinogi Y, Oh T. 2018. Simulating daily runoff in hydrologic standard basin considering agricultural reservoir operation. Journal of the Faculty of Agriculture, Kyushu University **63**(1), 119–130.

Philippines Historical Hazards. 2021. Climate change knowledge portal for development practitioners and policy makers. https://climateknowledgeportal.worldbank.org/country/philippines/vulnerability

Santillan JR, Ramos RV, David G, Recamadas SM. 2013. Development, calibration and validation of a flood model for Marikina River Basin, Philippines and its applications for flood forecasting, reconstruction, and hazard mapping.

Sevat E, Dezetter A. 1991. Selection of calibration objective function in the context of rainfall–runoff modeling in Sudanese savannah area. Hydrological Sciences Journal **36**, 307–330.

Soomro A, Babar M, Zaidi A, Ashraf A, Lund J. 2019. Sensitivity of direct runoff to curve number using the SCS-CN method. Civil Engineering Journal **5**, 2738–2746.

Syme B. 1990. Practical 1-D and 2-D computer modelling of flow and transport processes in rivers, estuaries and coastal waters. Queensland Division Technical Paper, 15–19.

World Health Organization (WHO). 2022. Floods. https://www.who.int/health-topics/floods#tab=tab_1